

Biogeosciences Discussions is the access reviewed discussion forum of *Biogeosciences*

A geochemical modelling study of the evolution of the chemical composition of seawater linked to a global glaciation: implications for life sustainability

G. Le Hir¹, Y. Godd ris², Y. Donnadi u¹, and G. Ramstein¹

¹LSCE, CNRS-CEA-UVSQ, Gif-sur-Yvette, France

²LMTG, CNRS, Observatoire Midi-Pyr n es, Toulouse, France

Received: 20 April 2007 – Accepted: 3 May 2007 – Published: 20 June 2007

Correspondence to: G. Le Hir (guillaume.le-hir@cea.fr)

1839

Abstract

The Snowball Earth theory initially proposed by Kirschvink (Kirschvink, 1992) to explain the Neoproterozoic glacial episodes, suggested that the Earth was fully ice-covered at 720 My (Sturtian episode) and 640 My (Marinoan episode). This succession of extreme climatic crises induced a stress which is considered as a strong selective pressure on the evolution of life (Hoffman et al., 1998). However recent biological records (Corsetti, 2006) do not support this theory as little change is observed in the diversity of microfossils outcrops before and after the Marinoan glacial interval. In this contribution we address this apparent paradox. Using a numerical model of carbon-alkalinity global cycles, we quantify several environmental stresses caused by a global glaciation. We suggest that during global glaciations, the ocean becomes acidic (pH~6), and unsaturated with respect to carbonate minerals. Moreover the quick transition from ice-house to greenhouse conditions implies an abrupt and large shift of the oceanic surface temperature which causes an extended hypoxia. The intense continental weathering, in the aftermath of the glaciation, deeply affects the seawater composition inducing rapid changes in terms of pH and alkalinity. We also propose a new timing for post glacial perturbations and for the cap carbonates deposition, ~2 Myr instead of 200 kyr as suggested in a previous modelling study. In terms of Precambrian life sustainability, seawater pH modifications appear drastic all along the glaciation, but we show that the buffering action of the oceanic crust dissolution processes avoids a total collapse of biological productivity. In opposite short-lived and large post-glacial perturbations are more critical and may have played a role of environmental filter suggested in the classic snowball Earth theory. Only a permissive life (prokaryotes or simple eukaryotes) may explain the relative continuity in microfossils diversity observed before, during and after Neoproterozoic glaciation events.

1840

1 Introduction

Oceans covered more than 75% of the Earth surface during the Neoproterozoic and were the only habitable environment for the Precambrian life. The history of the chemical composition of seawater is closely tied to the history of the atmosphere in terms of oxygen and carbon content, but also depends on the chemical signature of rivers entering into oceans and of hydrothermal fluids released in seawater along oceanic ridges. Reconstructions of the seawater composition during the geologic past rely on indirect data from marine sedimentary rocks. In consequence the global deposition of carbonate layers overlapping Neoproterozoic glacial deposits and the return of iron formations suggest strong changes in seawater composition at the end of the Proterozoic era (Hoffman and Schrag, 2002). Carbon isotopic anomalies in postglacial carbonates bring more credit to this hypothesis. Indeed the shift towards negative values recorded in those carbonates (Hoffman et al., 1998) is often considered as a biological productivity collapse, suggesting that the Precambrian life was deeply affected by a large environmental perturbation. All geological features cited previously might be explained by a common origin: a global glaciation, also known as the “snowball earth” event. However the biological record seems to show the contrary. A fine microfossils study of glacial intervals reveals no peculiar microbiota perturbations before and after Neoproterozoic glaciations (Corsetti et al, 2006). This inconsistency between the geological and biological records and the fact that a large environmental perturbation does not affect the biological diversity is surprising. Using a numerical model of the geochemical cycles we investigate this paradox by exploring perturbations of the chemical composition of the seawater during these extreme glacial events and in the direct aftermath. Based on the results, we explore the possible responses and survival of the living organisms to the global glaciation, and suggest possible links between late Proterozoic glaciations and biological evolution.

1841

2 Geological context and experimental design

The innovation of our study is to simulate the chemistry of the Proterozoic ocean all along the glaciation, and extending our modelling into post-glacial perturbations. Indeed previous modelling studies were only focused on the deglaciation (Higgins and Schrag, 2003), and authors used many assumptions on the oceanic state prevailing during the glaciation. To improve our knowledge of the ocean chemistry evolution during and after the glaciation, we build up a numerical model of the oceanic and atmospheric oxygen and carbon cycles, and alkalinity.

2.1 Initial assumptions

To investigate seawater perturbations during global glaciations, an important issue is to know whether the ocean remained in contact with the atmosphere during the whole glacial interval, or whether it was fully isolated. Patches of open water were proposed in the original Snowball Earth theory to keep the biosphere alive (Kirschvink, 1992). Also air-sea gas exchanges, through cracks in the sea-ice took place during the glaciation (Hoffman et al., 1998). Since tiny area of open waters allow efficient gas exchanges between the atmosphere and ocean (Le Hir et al., 2007¹), a scenario with the ocean and atmosphere in equilibrium during the glaciation appears the most likely solution. However, as the previous assumption remains partly speculative, we have performed a simulation with an isolated ocean so that both scenarios can be compared (uncertainties and limitations section).

If the ocean is not isolated from the atmosphere during the “snowball glaciation”, chemical evolutions of the two compartments are intertwined. In the absence of continental weathering, the main processes changing the seawater composition are those occurring at the seawater – oceanic crust interface. If we assume that the average hy-

¹Le Hir, G., Godd ris, Y., Donnadieu, Y., et al.: A scenario for the evolution of the atmospheric pCO₂ during a Snowball Earth, *Geology*, in review, 2007.

1842

drothermal water flux approaches 10^{13} m³/year (Elderfield and Schultz, 1996) then the whole oceanic volume will circulate into the oceanic crust in less than 1 million years (My). Considering that the minimal snowball duration exceeds 4 My (Bodiselsch et al., 2005), hydrothermal activity at mid-ocean ridges and low-temperature weathering of oceanic crust silicates would largely affect the seawater composition. These processes are thus considered in our modelling study.

2.2 Ocean interactions with the oceanic crust

2.2.1 The seafloor weathering process

The seafloor weathering is a carbon sink due to the dissolution of basaltic silicates (Alt and Teagle, 1999). In our model, the deep ocean is in contact with a water reservoir incorporated into the oceanic crust. Under the corrosive action of seawater, the reservoir of percolating waters is slowly depleted in carbon through low temperature dissolution of the basaltic crust. Indeed, the induced increase in alkalinity leads to the precipitation of carbonate minerals from highly saturated waters in vein inside the oceanic crust. This process removes carbon from the ocean atmosphere system at the million year timescale (Fig. 1), but does not influence the alkalinity budget since the net alkalinity flux is equal to zero. The global sink of carbon is estimated at 1.6×10^{12} moles/yr, at the lower end of the estimation performed by Alt and Teagle (1999) under present day conditions, but may increase with an oceanic acidification. To avoid any poorly constrained parameterization of this flux, we choose to estimate the weathering rate of the basaltic crust using laboratory kinetic laws for proton, OH⁻ and H₂O promoted dissolution.

$$R_{\text{bas}} = \sum_i k_i \cdot \exp\left(\frac{-E_i}{R \cdot T_p}\right) \cdot a_i^{n_i} \quad (1)$$

where the sum extends up to all the dissolving species (H⁺, OH⁻ and H₂O), while the index *i* stands for the dissolving species. E_i and k_i are respectively the activation

1843

energy and dissolution constant for each mineral depending on the species *i* promoted dissolution. These constants are taken from the WITCH model database (Godderis et al., 2006) or can be found in (Drever, 1997). T_p is the temperature of the percolating waters into the oceanic crust at which dissolution occurs. Here we fixed it at 313 K. a_i stands for the activity of the species *i* that promotes dissolution, and are calculated at each timestep of the simulation through carbonate speciation while n_i is the order of the dissolution reaction. The mineralogical composition of the oceanic crust is taken as the mineralogy of tholeiitic basalt (54% labradorite, 32% diopside, 9% basaltic glass, 4.3% apatite and 1.3% forsterite).

2.2.2 Hydrothermal fluxes at mid-ocean ridge (MOR)

The exact balance between the net emitted CO₂ flux at mid-oceanic ridges and CO₂ consumption through seafloor weathering is not known, meaning that we do not really know today whether oceanic ridges act as a CO₂ source or sink (Kerrick, 2001). In a conservative approximation, we assume a net MOR degassing of CO₂ into the deep ocean at a constant rate of 1.6×10^{12} moles/yr, which exactly balances the seafloor weathering, so that the overall interaction between the oceanic crust and the oceanic reservoir does not yield a net CO₂ flux under present-day conditions.

A consumption of O₂ by MOR systems through the formation of iron oxides and the precipitation of metalliferous sediments is included (Godderis et al, 2001). Assuming a mean water flux through on-axis MOR system of 420×10^{13} kg/yr (Elderfield and Schultz, 1996) and a complete removal of oxygen from circulating water, this sink reaches about 9×10^{11} moles/yr under present day conditions. It is then assumed to be simply proportional to the oxygen content of the percolating seawater. Finally, phosphorus is also removed through adsorption on hydrothermal plume particles in the vicinity of MOR systems at a present day rate of 1.4×10^9 moles/yr (Wallmann, 2003).

2.3 Geochemical modelling procedure

The geochemical model describes the time evolution of the carbon, oxygen, phosphorus and alkalinity geochemical cycles. It is a simplified and slightly modified version of the geochemical module of the GEOCLIM model (Donnadieu et al., 2006, Donnadieu et al., 2004, Godderis and Joachimski, 2004) (Fig. 2). The number of oceanic reservoirs has been reduced to two: one for the surface ocean and one for the deep ocean. Two reservoirs have been added below the deep ocean reservoir: the first one accounts for the water circulating into hydrothermal system at high temperature (350°C) while the second one describes the temporal evolution of the water percolating the oceanic crust along ridge flanks at low temperature (40°C). Carbonate speciation is calculated within each water reservoir as a function of the modelled alkalinity, total dissolved inorganic carbon and temperature of the waters. The ocean model is capped with an atmospheric reservoir. To simulate the initial seawater and atmospheric composition before the global glaciation, we first run the geochemical model according to Proterozoic pre-glacial conditions until a steady-state is reached. We use a standard silicate weathering law, where Ca^{2+} and Mg^{2+} weathering rates are proportional to global runoff and depend on mean global air temperature (Oliva et al., 2004), assuming the present silicate weathering consumes 13.2×10^{12} moles of atmospheric carbon per year (Dessert et al., 2003; Gaillardet et al., 1999). Continental carbonate weathering is proportional to global runoff times the concentration of Ca^{2+} in equilibrium with calcite minerals and atmospheric CO_2 at the calculated mean air temperature (Donnadieu et al., 2006). Global mean air temperature T_{air} (in °C) is assumed to be a function of atmospheric $p\text{CO}_2$ (ppmv):

$$T_{\text{air}} = 5.1339 * \ln(p\text{CO}_2) - 24.729 \quad (2)$$

This parametric relationship was obtained by running a radiative-convective climate model under Neoproterozoic conditions (solar constant = 1302 W/m^2 , mean global albedo = 0.3) for a variety of atmospheric CO_2 levels. Finally, continental runoff is assumed to be a simple function of global mean air temperature (Berner and Kothavala, 1845

2001).

Biological productivity in the surface ocean depends on (i) the incoming flux of phosphorus from the deep ocean, (ii) the weathering of continental surfaces (phosphorus flux is assumed to be proportional to runoff), and (iii) the seawater pH (Coleman and Colman, 1981). Since atmospheric oxygen level is thought to be around 10% of its present value (Kasting, 1987), we reduce the photosynthetic biological activity so that pre-glacial atmospheric O_2 stabilizes at 0.02 bar. Carbonate deposition F_{cd} occurs in the surface oceanic reservoir. Carbonate speciation is calculated at each time step, together with the saturation state of the oceanic waters Ω (Goddéris and Joachimski, 2004). Carbonate deposition is then calculated as following (Opdyke and Walker, 1992):

$$F_{cd} = k \cdot (\Omega - 1)^{1.7} \quad (3)$$

The inception of the global glaciation is simulated through an instantaneously shut down of all continental weathering fluxes as a consequence of the rapid growth of continental ice sheets. Surface water temperature is forced to drop from 20°C down to 26°C, and the vertical mixing, between surface and deep waters, decreases from $21 \times 10^6 \text{ m}^3/\text{s}$ to $0.2 \times 10^6 \text{ m}^3/\text{s}$ to represent a maximum oceanic circulation reduction. Then the model evolves freely. According to geological constrains, the maximal duration for the Marinoen glaciation event does not exceed 33 Myr (Zhou et al., 2004) (Condon et al., 2005). For this reason we performed a run wherein we impose a glaciation duration of 30 Myr.

3 Impacts of oceanic crust – seawater interactions during the glaciation

3.1 Quantification of mid oceanic ridge hydrothermal processes on seawater composition

A perturbation closely tied to submarine hydrothermal activity is the oxygen consumption by oxides formation. Prior to the onset of the snowball glaciation, and during the early phase of this glaciation, the deep ocean remains in the dysoxic domains at 0.025 mmol/kg, at a value close to the surface ocean value and constrained by the low atmospheric level (Fig. 3). Indeed, we reduced the biological productivity in the surface ocean to simulate a low atmospheric O₂ level prior to the glacial event. As a result, the reduced carbon flux down to the deep ocean is decreased, reducing the O₂ consumption required by its remineralization, resulting in the quasi absence of a vertical gradient in O₂. During the glaciation, the production of O₂ by photosynthesis and subsequent organic carbon burial rapidly goes down with the oceanic productivity. Indeed, phosphorus is rapidly consumed by hydrothermal processes due to its short residence time (10⁵ yrs), and the ocean rapidly lacks nutrients (within 1 million years after the beginning of the glaciation). Furthermore, the drastic reduction in vertical mixing leads to the lowering of the oxygenation of deep waters. As a consequence the oxygen consumption by hydrothermal activity overcomes the oxygen input at depth and enhances the anoxia of the deep ocean. In permanent contact with the atmosphere, the oxygen concentration of the surface ocean remains quasi-constant along the glacial interval, being only affected by the long term global exospheric O₂ reduction due to consumption in hydrothermal systems. A short oxygenation event is calculated at the inception of the glaciation. Due to the prescribed oceanic temperature decrease from 20°C down to 2°C, the oxygen solubility enhancement results in a rapid and short lived oxygen dissolution into the ocean.

The constant dissolution of atmospheric oxygen into the ocean through patches of open waters and its continuous consumption at mid oceanic ridges leads to a slow decrease in the atmospheric oxygen level. Within 30 Myr, the atmospheric pO₂ de-

1847

creases by 30%, which is not enough to generate a fully anoxic surface ocean. However the weakness of the vertical oceanic mixing allows the deep ocean to become quasi-anoxic. Therefore during the glaciation, the ocean tends to be “stratified” with a poorly oxygenated deep ocean (dissolved O₂ concentration of 10 μmol/kg and below) and dysoxic surface ocean (around 20 μmol/kg). This result can explain iron formation occurrences associated with glacial and post glacial deposits (Hoffman and Schrag, 2002; Young, 1992). Indeed the precipitation of iron formation (BIF) requires three conditions to be verified: (1) deep ocean anoxia, (2) low sulphur availability, and (3) surface-water oxygenated. Here, our model simulated a quasi-anoxic deep ocean with a dysoxic surface ocean, thus facilitating the precipitation of BIFs. Regarding sulphur availability, we can only speculate that the absence of weathering implies a shut down of riverine sulphate input, since no sulphur cycle is implemented. As a consequence, the iron formation reappearance during the glaciation remains plausible where upwelling currents carry reduced iron from the deep ocean, explaining their limited extension.

3.2 Carbon cycle evolution, seafloor weathering and carbonate dissolution

Before the glacial event, calculated seafloor weathering consumes 1.6×10^{12} carbon mol/year, the main carbon consumption being located on the continents through aerial silicate weathering (Fig. 4). During the glaciation, the growth of large ice sheets led to a collapse of the CO₂ consumption through continental weathering and biological carbon pumping, and consequently to the atmospheric CO₂ built up (Fig. 4). If the CO₂ is allowed to dissolve within the ocean during the building up of high atmospheric carbon levels, seawater pH should drastically decrease (Fig. 5) and promote both carbonates (Hoffman and Schrag, 2002) and oceanic basaltic crust dissolutions, both counteracting the pH decrease. However the absence of pelagic carbonates organisms before the Mesozoic (Bown, 2004; Kuznetsova, 2003) excludes the possibility to accumulate deep sea carbonates. The other source of alkalinity might have been the dissolution of carbonate precipitated on the continental platform prior to the glaciation. However

1848

the sea level drop induced by the global glaciation has certainly strongly reduced the availability of this carbonate reservoir for dissolution. Nevertheless, since carbonates are highly soluble when pH decreases below 8, it is worthy to estimate the maximum amount of carbonates that can be dissolved during the glacial event itself.

5 Carbonate dissolution is a function of the saturation state of the seawater with respect to carbonate minerals Ω . Once saturation is reached, dissolution stops. Dissolution F_{diss} can be described by the following equation as long as Ω stays below 1:

$$F_{\text{diss}} = k_{\text{diss}} \cdot (1 - \Omega)^{1.7} \quad (4)$$

10 where k_{diss} is a constant representing the dissolution flux of carbonate in mol/yr when undersaturation is complete ($\Omega=0$). The amount of carbonate that can be dissolved is thus strongly controlled by the saturation state of the ocean. Just after the onset of the global glaciation, Ω starts to decrease in response to the shut down of the continental weathering and the early stages of the CO_2 accumulation into the exospheric system. 15 Once Ω is below 1, dissolution of carbonate minerals begins, releasing two equivalent of alkalinity and one mole of carbon per mole of carbonate mineral. This dissolution counteracts further decrease in Ω , but also fixes the temporal evolution of F_{diss} . The k_{diss} constant can be seen as a restoring force counteracting any Ω decrease: the bigger it is, the stronger the buffering effect will be, and the closer to saturation will stay the seawater. 20 We found that the minimum value of k_{diss} required to stabilize seawater at $\Omega=1$ is equal to 10^{15} mol/year. Assuming this maximum buffering effect, we found that during the first 10 million years of the glacial event, $\sim 15 \times 10^{20}$ g of seafloor carbonate are dissolved. Assuming area of carbonate accumulation on shelves of $15 \times 10^6 \text{ km}^2$ prior to the snowball, which is a kind of a maximum value, corresponding to the Upper 25 Cretaceous environment (Walker et al, 2002), this carbonate mass would be 35 m thick. Considering the low availability of shelf carbonate during global glaciations (because of sea level drop), if only 1m of carbonate covers the same surface, then this carbonate mass will be dissolved in less than 1 Ma after the beginning of the glaciation. Furthermore, even the dissolution of 15×10^{20} g during the first 10 million years does not

1849

compensate for the pH decrease (Fig. 6). Therefore we claim that carbonate dissolution cannot counteract the deep acidification of seawater during a snowball event. As a result, carbonate dissolution was probably not an efficient buffer of the pH decrease, and the seawater acidification enhances the consumption of dissolved carbon 5 through low temperature alteration of the oceanic basaltic crust. The CO_2 consumption through seafloor basaltic weathering rises until the ocean is sufficiently acidified (Fig. 5) so that seafloor weathering balance the prescribed total solid Earth outgassing (8.65×10^{12} mol/year) (Fig. 4).

10 Therefore along the glacial interval, the massive atmospheric CO_2 dissolution into the ocean acidifies the seawater, forcing the ocean to be undersaturated with respect to carbonate minerals. However oceanic crust interactions with the deep ocean partly buffer its acidification, maintaining seawater pH around 6, while it goes below this threshold in the absence of seafloor weathering (Fig. 5).

4 Seawater properties aftermath to the glaciation

15 4.1 Post glacial warming duration and seawater hypoxia

The cap carbonates overlapping glacial diamictites shows a “knife-edge” contact suggesting no significant hiatus. This abrupt juxtaposition implies an instantaneous shift from ice-house to extreme green-house conditions. Geological and modelling studies estimate that this transition could have lasted between 100 years (Halverson et al., 20 2004) and 10 kyr (Higgins and Schrag, 2003). The melting of the snowball Earth is the result of the mega greenhouse effect induced by a high atmospheric CO_2 mixing ratio. Even if uncertainties remain on the pCO_2 required to overcome the high albedo of snowball Earth, Pierrehumbert modelling study (Pierrehumbert, 2005) demonstrates that this value overcomes 0.2 bar and might be equal to 0.29 bar.

25 Our model prescribes the termination of the glaciation after 30 Myr, which leads to a final pCO_2 level reaching 0.26 bar, a value close to the melting threshold estimate.

1850

Once the melting of the ice completed, such high $p\text{CO}_2$ value induces a large warming effect (Fig. 6). The surface temperature shifts from 275 K to ~ 310 K in a few 10^4 years. This sudden and extreme warming further enhances the dysoxia in seawater, since solubility of O_2 coevally decreases, and oxygen concentration in surface waters falls from 24.4 down to $11.4 \mu\text{mol/kg}$.

With ice meltdown, the continental surface reappears. Warm temperatures and large runoff calculated in the aftermath to the glaciation result in a strong continental weathering. CO_2 consumption by continental silicate rock weathering rises up by a factor of 7 compared to present day values (Fig. 7). This increase, combined with the restart of the carbonate burial engine, results in a quick decline of CO_2 and a return toward initial conditions in ~ 3 Ma, a duration longer than 200 ky previously estimated (Higgins and Schrag, 2003) (see Table 1).

4.2 The termination of an acidic ocean and the deposition of the cap carbonates: origin and timing.

Since carbonates are highly soluble in an acidic ocean, the carbonate reappearance could be interpreted as the termination of the acidic ocean prevailing during the glaciation. Carbonates immediately capping the glacial deposits are supposed to be formed by the rapid continental carbonate weathering in the direct aftermath of the snowball, and are usually interpreted as a transgressive unit precipitated during the sea level rise. Indeed, field observations (Hoffman and Schrag, 2002) show that Marinoan cap carbonates are transgressive. Nevertheless, it should be noted that most Sturtian cap carbonates are formed after the post-glacial transgression (Hoffman and Schrag, 2002; Shield, 2005).

Under direct post glacial conditions (acid rains induced by 0.26 bars of CO_2 , intense runoff and warm temperatures), our thermodynamic model for carbonate dissolution predicts a carbonate weathering rate peaking at $\sim 2.1 \times 10^{14}$ mol of Ca^{2+}/yr (4 times the pre-glacial value, see Fig. 7), a flux large enough to accumulate a carbonate bank of 45m thickness on the whole continental shelf area (15.10^6 km^2) in only 10 kyr.

1851

Therefore, the mass of carbonate coming from the post-glacial carbonate weathering is largely enough to lead to the precipitation of the cap carbonates.

However additional conditions are required for carbonates to precipitate: seawater must return to saturation with respect to carbonate minerals. After the melting of the ice sheets, the post glacial ocean display a pH of 6, and a saturation ratio Ω virtually equal to 0. Even if large amounts of Ca^{2+} and HCO_3^- are released from the continents into the ocean, it takes time to balance the initial acidity. As shown in Fig. 8, the ocean needs 20kyr to restore saturation ($\Omega > 1$) through the high flux of alkalinity coming from continental weathering. In our model, the precipitation of cap carbonates occurs, not immediately but almost at the geological timescale, i.e. 20 kyr after the deglaciation. Regarding the sedimentological context of the cap carbonates, the duration of the sea level rise appears important. Indeed, if the sea level rise occurs in more than 20 kyr, then our modelled cap carbonates precipitate in a transgressive context, in agreement with the Marinoan data (Hoffman and Schrag, 2002). Conversely, duration shorter than 20 kyr would induce non transgressive cap carbonates. A classic estimation based on Quaternary ice-sheets meltdown is 10 kyr. However, inferring Quaternary duration within the snowball context is difficult, and it is reasonable to ask questions on this analogy. Indeed the shift towards a super greenhouse climate should promote a rapid melting, but the amount of ice locked on the continent during a snowball Earth has been evaluated around 200 millions of km^3 (Donnadieu et al., 2003) which is four time the amount of ice melted in 10 kyr between the Last Glacial maximum and the interglacial.

4.3 Isotopic records of $\delta^{13}\text{C}$ in cap carbonates

Cap carbonates are a key element of the snowball theory and many discussions were focused on their origin, and the significance of seawater $\delta^{13}\text{C}$ they recorded. A fine description of the cap carbonate succession reveals two units (Hoffman and Schrag, 2002): a basal unit of cap dolostone with an initial $\delta^{13}\text{C}$ of -2‰ and a subsequent unit of limestone with a $\delta^{13}\text{C}$ tending toward 0‰ (Higgins and Schrag, 2003). The dolostone-limestone transition is characterized by a $\delta^{13}\text{C}$ of -4‰ (Higgins and Schrag,

1852

2003; Hoffman and Schrag, 2002). A previous geochemical model study by Higgins & Schrag (2003) focused on post glacial isotopic records suggesting that the basis of cap carbonate deposition is driven by alkalinity input from carbonate weathering. They also assumed that the negative $\delta^{13}\text{C}_{\text{carb}}$ trend observed in dolostones was induced by surface temperature and the saturation state of the ocean. The main weakness of this study is the lack for constraint on the snowball ocean, since all calculations start at the melting of the ice. The results are thus highly dependant on initial conditions for the $\delta^{13}\text{C}$ of the ocean-atmosphere system, and the saturated state of the ocean just after the melting of the snowball. Here we calculate the time evolution of the ocean during the snowball event (including $\delta^{13}\text{C}$ and saturation state), thus fully relaxing the initial pre-glacial conditions, prior to explore the direct post glacial ocean.

During the snowball glaciation, the building of a high DIC reservoir in the ocean while alkalinity remains fixed as a result of continental weathering shutdown induces a shift of the main dissolved carbon species from HCO_3^- to H_2CO_3 . The collapse of biological productivity slowly decreases the $\delta^{13}\text{C}$ of DIC to mantle values (-4‰ Fig. 9a). Because H_2CO_3 is depleted in ^{13}C , HCO_3^- and CO_3^{2-} display rather high $\delta^{13}\text{C}$ during the glacial phase in order to maintain the ^{13}C balance (see the green curve on Fig. 9a). It is interesting to mention that DIC $\delta^{13}\text{C}$ goes below the mantle value during the glaciation to -6‰ when accounting for the sea floor weathering (red line on Fig. 9a) whereas it reaches only -3‰ without sea floor weathering (black line Fig. 9a). This result is linked to the carbon sink that consumes carbon at the $\delta^{13}\text{C}$ value of CO_3^{2-} , thus inducing a fractionation and further removing ^{13}C from the seawater (Fig. 9a). As a consequence, the $\delta^{13}\text{C}$ of CO_3^{2-} at the end of the snowball Earth is at $+1.2\text{‰}$ (Fig. 9b). Then the restart of continental weathering, the deacidification of seawater and the rise in temperature decrease this value down to -4‰ within 10^5 years after the melting, followed by a slow recovery to pre-glacial values within 2 to 3 million of years.

The comparison between our result and isotopic records in cap carbonates suggests that the most negative peak in $\delta^{13}\text{C}$ (i.e. -4‰) appears 80 kyr after the onset of the deglaciation and is coeval with the transition from cap dolostone to limestone (Fig. 9b).

1853

Since the ocean was undersaturated during the first 20 kyr after the deglaciation, it explains the absence of recorded positive $\delta^{13}\text{C}_{\text{carb}}$ values just after the glaciation termination. Indeed, the first carbonate being deposited displays a calculated $\delta^{13}\text{C}$ of -2‰ in good agreement with the $\delta^{13}\text{C}$ profile measured across the cap carbonates.

These results are qualitatively in agreement with previous calculations (Higgins and Schrag, 2003), but the timing is drastically different. In the Higgins and Schrag study, deglaciation starts with 0.12 bars of atmospheric CO_2 , and the authors assumed that this high level of CO_2 is consumed in only 200 kyr. In the present simulations, it takes respectively 3 and 2 million years to consume the 0.26 and 0.12 bars of post-glacial CO_2 through silicate continental weathering (Fig. 7). Based on the ^{13}C output displaying the return to the pre-glacial of $+4\text{‰}$ only after 2 Ma (Fig. 9b). Correlations with Ghaub Formation (Hoffman et al., 1998) suggest that the timing of cap carbonate deposition may be longer than initially suggested, 400 kyr instead of 200 kyr (Fig. 9b). This longer timespan for deposition is in agreement with the existence of multiple magnetic reversals inside the first 20 m of the Puga cap carbonate sequence in Brazil (Trindade et al., 2003).

5 Discussion

The Earth system undergoes large environmental perturbations at the end of the Proterozoic, but surprisingly, it seems that the evolution of life was not largely perturbed during the same time interval. Complex organisms are known before and after the glacial interval (Corsetti et al., 2006) suggesting that the biosphere must have survived. Biological studies show that silicified microfossils from pre and syn-glacial units reveal weak changes. Similarly the glacial events seem to have been innocuous for acritarchs, since the Australian record reveals no change in diversity throughout the glacial event (Corsetti et al., 2006).

Here we have quantified environmental stresses during and aftermath to a snowball Earth. Our geochemical model shows that the oceanic environment was submitted

1854

to large and long term perturbations during the glaciation. After 30 Myr of glaciation, the ocean was cold, acidic, undersaturated with respect to carbonate minerals, dysoxic above 100m, and anoxic at depth. Maintenance of life under this environment is difficult to assess.

5 The closest analog to Neoproterozoic Snowball Earth environment may be landfast sea ice in the modern-day polar regions. Under a thick sea ice, perennial microbial mats survive in association with a large biota, polar regions being sites wherein a large diversity of organisms is maintained (protists, metazoa or bacteria). Cyanobacteria communities existing in a cold environment show an extreme tolerance to low temperature (Vincent and Howard-Williams, 2000) even if their growth appears limited (Price and Sowers, 2004). Moreover as large populations of microscopic organisms can fit in a small surface wherein the light remains available, they can preserve a relative diversity even if small oasis remain. Therefore cold temperatures and sea-ice extension were probably not the worse environmental forcing, but the snowball ocean was also acidic. Since Neoproterozoic primary producers were cyanobacteria, we focused on their photosynthetic efficiency as a function of acidification (Coleman and Colman, 1981). Based on biotic response of present day living cyanobacteria, the primary production is reduced as pH goes down (Fig. 10), and fully collapses around pH 5, thus below the minimum seawater pH during the glaciation. Moreover the slow drop of the photosynthesis activity as a function of declining pH is not in agreement with an abrupt extinction. The snowball ocean was possibly characterized by weak primary production, limited by low temperature and low pH, while the dysoxic conditions prevailing in the surface waters were not different compared to the oxic state of the photic zone prior to the snowball.

25 Our results suggest that the most important environmental pressure occurred during the deglaciation, and not during the snowball event itself. At the termination of the glaciation the ocean becomes warm, hypoxic and reaches a neutral pH in 20ky, an extremely short time span in response to the restart of the continental inputs through weathering. If the modern biosphere has to be submitted to such fast environmental

1855

changes, it will be probably removed from the Earth surface, however, it appears to be not the case during the Neoproterozoic glacial events (Corsetti et al., 2006). Nevertheless, as suggested by Hoffman et al. (1998), the prokaryotic biosphere dominating the Neoproterozoic ecosystem is more permissive than eukaryotes when submitted to extreme environment stresses. Considering their physiology and ability to survive in extremely diverse environments, prokaryotes organisms could endure a large range of variability because they need less energy to ensure their fundamental functions. Therefore prokaryotes and other simple organisms (acritarchs, algae) may have been less affected by strong environmental fluctuations, and this may explain their relatively continuous diversity before, during and just after the glaciation. However, such assumption deserves more studies on the response of Neoproterozoic like organisms to seawater chemistry and physical properties changes; as well as micropaleontological studies of the Neoproterozoic sedimentary rocks.

6 Uncertainties and limitations

15 Most of our results partly depend on the assumption that the ocean and atmosphere are in contact through cracks in the sea ice, and that gas exchange is fast enough so that the ocean and atmosphere are close to equilibrium with respect to each other. Sea-ice thickness estimates for a globally ice-covered Earth largely depend on the model of ice dynamic used (Goodman and Pierrehumbert, 2003; Pollard and Kasting, 2005; Warren et al., 2002). The maximum thickness has been estimated around one kilometer in the tropics and several kilometers in middle latitudes. Such a thick sea-ice may limit the crack propagation, and thus reduce the gas exchanges between the atmosphere and ocean. However, the existence of emerged hydrothermal area through melting of the sea ice may still allow gas exchanges. Nevertheless, an isolated scenario cannot be a priori excluded, and we performed a simulation assuming no exchanges between the atmosphere and the ocean.

25 In an isolated ocean, the oxygen level drops very quickly in the surface and deep

1856

waters. The hydrothermal sink entirely consumes the oxygen available in the ocean within 1 Myr. Furthermore, the accumulation of carbon in the ocean is now limited to the degassing at mid-oceanic ridges, and the seafloor weathering rapidly buffer the pH decrease, keeping it around 8 (Fig. 11). However, this result is totally dependent on the relative importance of MOR degassing and consumption of carbon through seafloor weathering (assumed to be balanced at 1.5×10^{12} moles/yr today) (Alt and Teagle, 1999). Since no atmospheric CO_2 is dissolved into the ocean, atmospheric CO_2 level reaches 0.26 bar in only 7 Ma instead of 30 Ma (Fig. 11). At the termination of the glaciation, the massive atmospheric CO_2 dissolution induces huge and rapid perturbation for pH, dropping from 8 to 6 in only 10 kyr. In this context the oceanic pH is not buffered by the carbonate weathering because the atmospheric carbon dissolution rate is faster and much more important. Therefore an isolated ocean is not a solution to reduce environmental perturbation in the aftermath of the glaciation, since post-glacial modifications are even stronger compared to a simulation where the ocean and atmosphere are kept in contact all along the glaciation.

Many other uncertainties still remain. One of the most important is the behaviour of weathering fluxes during the deglaciation. We have extrapolated to the super greenhouse climate, parametric laws describing CO_2 consumption through continental silicate weathering as a function of air temperature and runoff that were estimated for the present day climatic conditions (Oliva et al., 2003). As a result, silicate weathering rises 7 times above its present day value, and controls the rate at which the super greenhouse climate is finally buffered. This is a first order study, and future work should use more complex model for estimating weathering rates. For carbonate rocks, we used a simple thermodynamic model assuming equilibrium of the continental waters with atmospheric CO_2 at the model air temperature (Donnadieu et al., 2006). Although this method also suffers from poorly constrained parameters, such as the area of carbonate outcrops by the time of the deglaciation, it is more efficient than extrapolating parametric laws calibrated for present day conditions. A thermodynamic and kinetic method might be similarly applied to estimate silicate weathering rates in future studies.

1857

Finally, the accumulation of cap dolostones is still problematic. Since mid-oceanic ridges act as huge rock-fluid ion exchange system for Ca^{2+} and Mg^{2+} , Ca^{2+} being released to the fluid and Mg^{2+} being consumed by the conversion of oceanic basalt into amphibolites, then without any inputs from rivers, the Mg/Ca ratio only depends on the hydrothermal activity. Our model simulates that the ocean tends to become calcitic (Mg/Ca ratio ~ 1.4) just before the deglaciation suggesting that carbonates immediately capping the glacial deposits should be calcite. However geological records show that first carbonate precipitated are primary dolomite ($\text{Ca}_{0.5}\text{Mg}_{0.5}\text{CO}_3$), indicating a rather high Mg/Ca ratio in seawater at the time of deposition. Therefore the seawater composition must have deeply changed in the direct aftermath of the glaciation to allow precipitation of primary dolomite. Moreover estimates of the dolomite abiotic precipitation rate (Pokrovsky and Schott, 2001) shows that the kinetics of the reaction is by far too low to account for the cap dolostone mass. Obviously, cap dolostone were accumulated through the mediation of microbial activity, as they contain non negligible amount of organic matter (Elie et al., 2007). Present day area of dolomite accumulation are located in dysoxic environment and in the presence of sulfate reducing bacteria only, at rates potentially much faster than abiotic precipitation rate. Because of this complexity, we have to assume that cap dolostone precipitation rate behaves as calcite precipitation rates, which is not correct. The enigma of the dolostone precipitation in the aftermath of the snowball will not be solved until present day analog have been fully explored and understood.

7 Conclusions

During a global glaciation, the sea-ice growth reduces the oceanic life habitat and the population size of species depending on the light availability. The absence of an efficient carbonate dissolution associated with high atmospheric pCO_2 levels (up to 0.26 bars) progressively acidifies the ocean down to pH 6, accounting for the buffering effect of seafloor basalt dissolution. Coevally overturning reduction and oxygen

1858

consumption by hydrothermal vents produce a dysoxic ocean in surface and anoxic at depth. The glacial ocean also rapidly becomes fully undersaturated with respect to carbonate minerals.

Once the threshold for the melting of the snowball Earth is reached, the exospheric system undergoes rapid and dramatic changes. During the first 20 kyr, the ocean becomes warm, hypoxic, and remains too acidic and undersaturated to allow for sedimentary carbonate accumulation. Then the ocean becomes saturated enough and cap carbonate accumulation is eventually allowed. Starting with a calculated $\delta^{13}\text{C}$ of -2‰ their isotopic signature falls to -4‰ within the first 100 kyr, then goes back to the pre-glacial of $+4\text{‰}$ within 2 Ma. This sequence suggests a longer time-span for cap carbonate accumulation (about 400 kyr) compared to previous estimate (200 kyr).

The most important environmental stress for life does not occur during the glaciation event itself, but rather during the onset and removal of the super greenhouse effect in the aftermath of the glaciation. Indeed, pH decrease from 8 to 6 during the snowball event spans about 4 Ma, mainly during the early stages of the glacial event. But pH comes back from 6 to 8 within 20 kyr during the super greenhouse effect, together with a sharp increase in temperature and the development of widespread anoxia.

We are aware that many other processes may resolve the apparent paradox between biological and geological records. However, environmental forcing associated with snowball events quantified in this paper may explain bio-geological evidence. Since prokaryotes are more permissive than eukaryotes when undergoing stresses, snowball Earth perturbations support the hegemony of prokaryotes versus eukaryotes all along the end of Precambrian. This selective advantage of prokaryotes might explain why complex organisms have waited a long period of time after snowball events to overcome the prokaryotic organisms and to become more abundant in geological records.

Acknowledgements. This work was achieved thanks to the financial support of the CEA and the CNRS through the Eclipse program "Comprendre et modéliser la planète Terre" and in collaboration with the Climate Systems Center, which receives funding from the U.S. National

1859

Science Foundation under grant ATM-0121028.

References

- Alt, J. C. and Teagle, D. A. H.: The uptake of carbon during alteration of ocean crust. *Geochimica Et Cosmochimica Acta*, 63(10), 1527–1535, 1999.
- Berner, R. A. and Kothavala, Z.: GEOCARB III: A revised model of atmospheric CO₂ over phanerozoic time, *Am. J. Sci.*, 301(2), 182–204, 2001.
- Bodiseltsch, B., Koeberl, C., Master, S., and Reimold, W. U.: Estimating duration and intensity of Neoproterozoic snowball glaciations from Ir anomalies, *Science*, 308(5719), 239–242, 2005.
- Bown, P. R., Lees, J. A., and Young, J. R.: In *Coccolithophores-From molecular processes to global impact*, edited by: Thierstein, H. R. and Young, J. R, Springer Verlag, 481–505, 2004.
- Coleman, J. R. and Colman, B.: Inorganic carbon Accumulation and Photosynthesis in a Blue-green Alga as a Function of external pH, *Plant Physiology*, 67, 917–921, 1981.
- Condon, D., Zhu, M. Y., Bowring, S., et al.: U-Pb ages from the neoproterozoic Doushantuo Formation, China, *Science*, 308(5718), 95–98, 2005.
- Corsetti, F. A., Olcott, A. N., and Bakermans C.: The biotic response to Neoproterozoic snowball earth. *Paleogeography, Paleoclimatology, Paleoecology*, 232, 114–130, 2006.
- Dessert, C., Dupre, B., Gaillardet, J., et al.: Basalt weathering laws and the impact of basalt weathering on the global carbon cycle. *Geochimica Et Cosmochimica Acta*, 69(10), A687–A687, 2003.
- Donnadieu, Y., Fluteau, F., Ramstein, G., Ritz, C., and Besse, J.: Is there a conflict between the Neoproterozoic glacial deposits and the snowball Earth interpretation: an improved understanding with numerical modeling, *Earth Planet. Sci. Lett.*, 208(1–2), 101–112, 2003.
- Donnadieu, Y., Godderis, Y., Ramstein, G., Nedelec, A., and Meert, J.: A "snowball Earth" climate triggered by continental break-up through changes in runoff, *Nature*, 428, 303–306, 2004.
- Donnadieu, Y. Godderis, Y., Pierrehumbert, R., et al.: A GEOCLIM simulation of climatic and biogeochemical consequences of Pangea breakup, *Geochem. Geophys. Geosyst.*, 7, 2006.
- Drever, J. I.: *The Geochemistry of natural waters*, Prentice Hall, 436 pages, 1997.

1860

- Elderfield, H. and Schultz, A.: Mid-ocean ridge hydrothermal fluxes and the chemical composition of the ocean, *Ann. Rev. Earth Planet. Sci.*, 24, 191–224, 1996.
- Elie, M., Nogueira, A. C. R., Nédélec, A., Trindade, R. I. F., and Kenig, F.: Biodiversity collapse and red algal bloom in the aftermath of the Marinoan Snowball Earth, *Terra Nova*, accepted, 2007.
- 5 Gaillardet, J., Dupre, B., Louvat, P., and Allegre, C. J.: Global silicate weathering and CO₂ consumption rates deduced from the chemistry of large rivers, *Chem. Geol.*, 159(1–4), 3–30, 1999.
- Godderis, Y., Francois, L. M., and Veizer, J.: The early Paleozoic carbon cycle, *Earth Planet. Sci. Lett.*, 190(3–4), 181–196, 2001.
- 10 Godderis, Y. and Joachimski, M. M.: Global change in the Late Devonian: modelling the Frasnian-Famennian short-term carbon isotope excursions, *Palaeogeogr. Palaeoclimatol. Palaeoecol.*, 202(3–4), 309–329, 2004.
- Godderis, Y., Francois, L. M., Probst, A., Schott, J., Moncoulon, D., Labat, D., and Viville, D.: Modelling weathering processes at the catchment scale: The WITCH numerical model, *Geochimica Et Cosmochimica Acta*, 70(5), 1128–1147, 2006.
- 15 Goodman, J.C. and Pierrehumbert, R. T.: Glacial flow of floating marine ice in “Snowball Earth”, *J. Geophys. Res.-Oceans*, 108(C10), doi:10.1029/2002JC001471, 2003.
- Halverson, G. P., Maloof, A. C., and Hoffman, P. F.: The Marinoan glaciation (Neoproterozoic) in northeast Svalbard, *Basin Res.*, 16(3), 297–324, 2004.
- 20 Higgins, J. A. and Schrag, D. P.: Aftermath of a snowball Earth, *Geochem. Geophys. Geosyst.*, 4, 2003.
- Hoffman, P. F., Kaufman, A. J., Halverson, G. P., and Schrag, D. P.: A Neoproterozoic snowball earth, *Science*, 281(5381), 1342–1346, 1998.
- 25 Hoffman, P. F. and Schrag, D. P.: The snowball Earth hypothesis: testing the limits of global change, *Terra Nova*, 14(3), 129–155, 2002.
- Kasting, J. F.: Theoretical Constraints On Oxygen And Carbon-Dioxide Concentrations In The Precambrian Atmosphere, *Precambrian Res.*, 34(3–4), 205–229, 1987.
- Kerrick, D. M.: Present and past nonanthropogenic CO₂ degassing from the solid Earth, *Rev. Geophys.*, 39(4), 565–585, 2001.
- 30 Kirschvink, J. L.: Late proterozoic low-latitude glaciation: the snowball earth. in the Proterozoic Biosphere, edited by: Schopf, J. W. and Klein, C., 51–52, 1992.
- Kuznetsova, K. I.: The first genera of planktonic foraminifers: Morphogenesis, development,

1861

- and expansion in the Jurassic, *Paleontological J.*, 37(5), 472–485, 2003.
- Oliva, P., Dupre, B., Martin, F., and Viers, J.: The role of trace minerals in chemical weathering in a high-elevation granitic watershed (Estibère, France): Chemical and mineralogical evidence, *Geochimica Et Cosmochimica Acta*, 68(10), 2223–2243, 2004.
- 5 Opdyke, B. N. and Walker, J. C. G.: Return Of The Coral-Reef Hypothesis – Basin To Shelf Partitioning Of CaCO₃ And Its Effect On Atmospheric CO₂, *Geology*, 20(8), 733–736, 1992.
- Pierrehumbert, R. T.: Climate dynamics of a hard Snowball Earth, *J. Geophys. Res.*, 110, D01111, doi:10.1029/2004JD005162, 2005.
- Pokrovsky, O. and Schott, J.: Kinetics and Mechanism of dolomite dissolution in neutral to alkaline solutions revisited, *Am. J. Sci.*, 301, 597–626, 2001.
- 10 Pollard, D. and Kasting, J. F.: Snowball Earth: A thin-ice solution with flowing sea glaciers, *J. Geophys. Res.-Oceans*, 110(C7), C07010, doi:10.1029/2004JC002525, 2005.
- Price, P. B. and Sowers, T.: Temperature dependence of metabolic rates for microbial growth, maintenance, and survival. *Proceedings Of The National Academy Of Sciences Of The United States Of America*, 101(13), 4631–4636, 2004.
- 15 Shield, G. A.: Neoproterozoic cap carbonates: a critical appraisal of existing models and the plume-world hypothesis, *Terra Nova*, 17(4), 299–310, 2005.
- Trindade, R. I. F., Font, E., D’Agrella, M. S., Nogueira, A. C. R., and Riccomini, C.: Low-latitude and multiple geomagnetic reversals in the Neoproterozoic Puga cap carbonate, Amazon craton, *Terra Nova*, 15(6), 441–446, 2003.
- 20 Vincent, W. F. and Howard-Williams, C.: Life on snowball Earth, *Science*, 287(5462), 2421–2421, 2000.
- Walker, L., Wilkinson, B. H., and Ivany, L. C.: Continental drift and Phanerozoic carbonate accumulation in shallow-shelf and deep-marine settings, *J. Geol.*, 110(1), 75–87, 2002.
- 25 Wallmann, K.: Feedbacks between oceanic redox states and marine productivity: A model perspective focused on benthic phosphorus cycling, *Global Biogeochem. Cycles*, 17(3), 1084, doi:10.1029/2002GB001968, 2003.
- Warren, S. G., Brandt, R. E., Grenfell, T. C., and McKay, C. P.: Snowball Earth: Ice thickness on the tropical ocean, *J. Geophys. Res.-Oceans*, 107(C10), 3167, doi:10.1029/2001JC001123, 2002.
- 30 Young, G. M.: Neoproterozoic Glaciation In The Broken-Hill Area, New-South-Wales, Australia, *Geological Society Of America Bulletin*, 104(7), 840–850, 1992.
- Zhou, C. M., Tucker, R., Xiao, S., et al.: New constraints on the ages of neoproterozoic glacia-

1862

Table 1. Post glacial weathering fluxes.

Continental weathering	$t_0 + 10$ kyr Deglaciation	$t_0 + 100$ kyr	$t_0 + 200$ kyr	$t_0 + 400$ kyr	$t_0 + 1$ Ma	$t_0 + 2$ Ma
Carbonate (in 10^{15} g/yr)	5.72	5.18	5.07	4.99	4.29	2.89
Silicate (in 10^{15} g/yr)	1.35	1.18	1.16	1.13	0.93	0.56

Higgins and Schrag (Higgins and Schrag, 2003) – total weathering used 17, 10 or 5 (in 10^{15} g/yr).

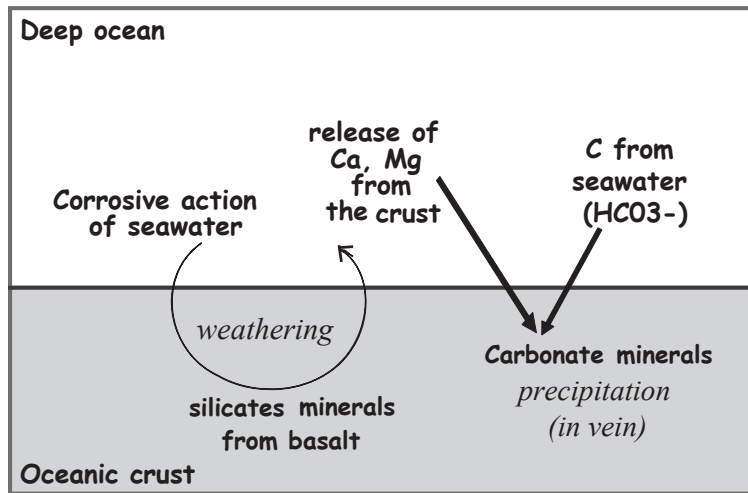


Fig. 1. Seafloor weathering is a carbon sink. Under the corrosive action of seawater, the percolating water consumes carbon by low temperature dissolution of basaltic crust. Seawater acidification enhances the corrosive ability of seawater.

1865

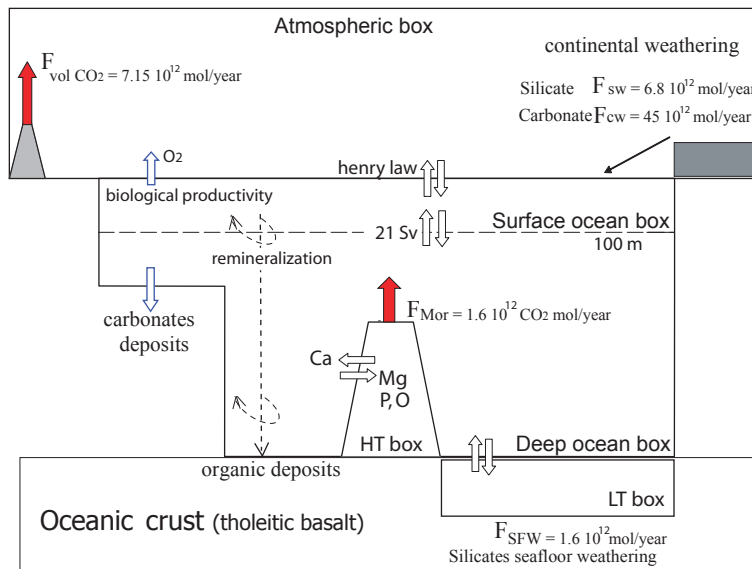


Fig. 2. geochemical model including oxygen carbon cycle and major cations behaviour. LT box (for Low Temperature) is used to represent interactions between the deep ocean and oceanic crust occurring at low temperature (313K). Innovation added in this box is the seafloor weathering process. HT box (for High Temperature) represents phenomena occurring between the deep ocean and hydrothermal vents at high temperature (cations exchanges and CO_2 release). Red arrows represent carbon sources. In snowball Earth conditions, we fix the ocean temperature at 2°C instead of 20°C and the overturning between the deep and surface ocean is reduced to 0.21 Sv. Due to ice-sheet growth, the continental weathering is cut off along the glaciation and in the common case wherein the atmosphere and ocean remain in equilibrium, the ice free oceanic surface is reduced at 3600 km^2 , the minimal surface requires for an efficient diffusion between the atmosphere and ocean.

1866

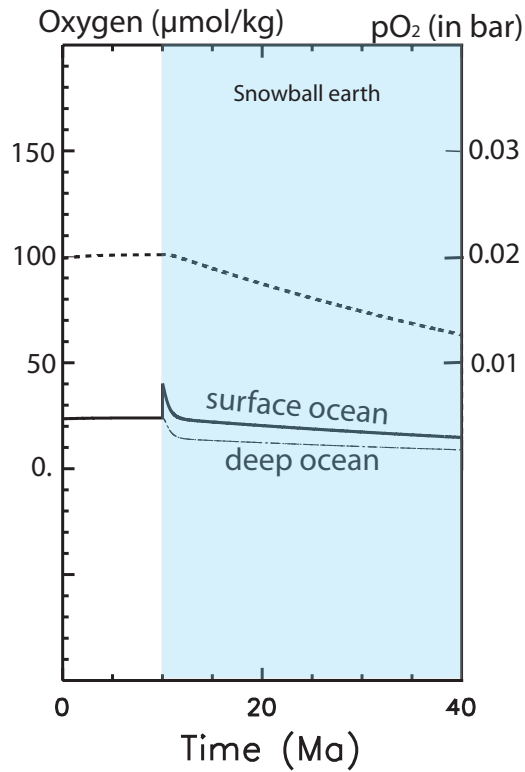


Fig. 3. Oxygen mixing ratio along the glaciation with an ocean and atmosphere in steady state. The dash line represents the atmospheric O_2 mixing ratio, black lines being the surface and deep ocean oxygen concentrations. The blue bland represents the glaciation duration.

1867

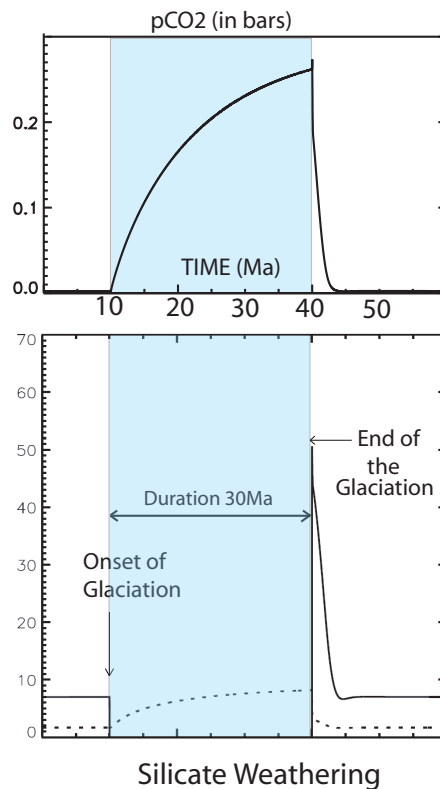


Fig. 4. CO_2 evolution as a function of the snowball earth duration and silicate weathering flux (in 10^{12} mol/yr) respectively due to continental weathering (black line) and seafloor weathering (dash line). The blue bland represents the glaciation duration.

1868

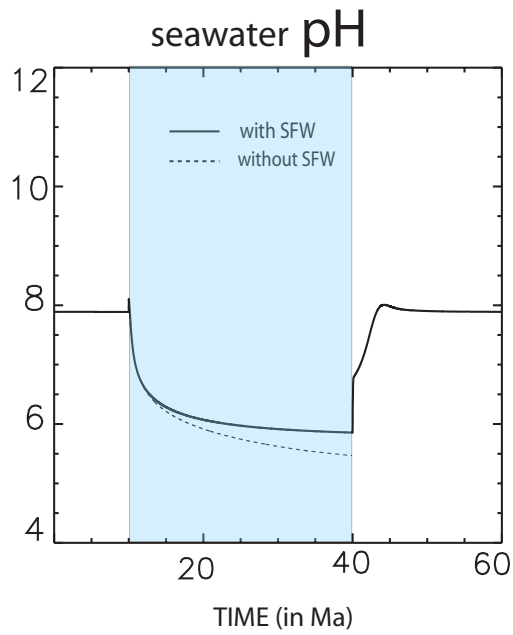


Fig. 5. Oceanic pH evolution during the glaciation. Snowball Earth begins after 10 Ma and lasts 30 Ma. All runs show that during a snowball event the seawater pH tends towards acidic values. Since the seafloor weathering (SFW) is enhanced by the seawater acidification, this process consumes enough CO_2 to stabilize the quantity of carbon dissolved into the ocean, which buffers the pH. The blue bland represents the glaciation duration.

1869

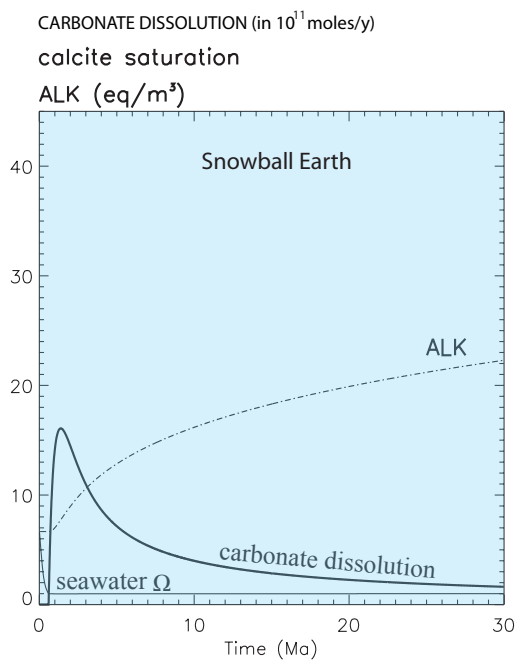


Fig. 6. Evolution of the seawater omega and alkalinity along a snowball Earth (duration 30 Ma). The carbonate dissolution is efficient enough to stabilize the omega at 1. The blue bland represents the glaciation duration.

1870

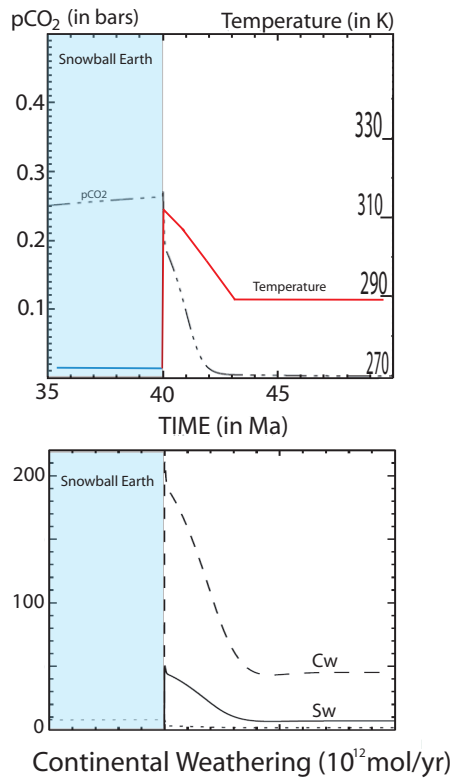


Fig. 7. Temperature, pCO₂ and weathering flux in the aftermath of the glaciation. The blue bland represents the glaciation duration. C_w is for Carbonate Weathering rate (dash line) and S_w for Silicate Weathering (black line).

1871

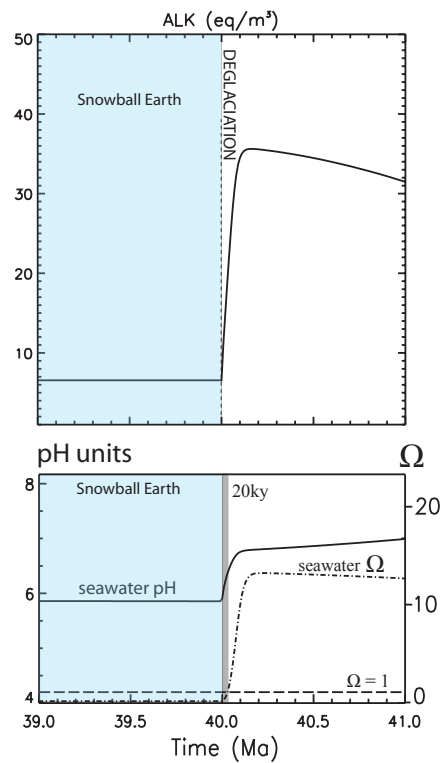


Fig. 8. Seawater saturation the termination of the glaciation (occurring at 40 Ma). The blue bland represents the glaciation duration. The grey band shows the minimum time (20 kyr) to reach the saturation after the termination of the glaciation

1872

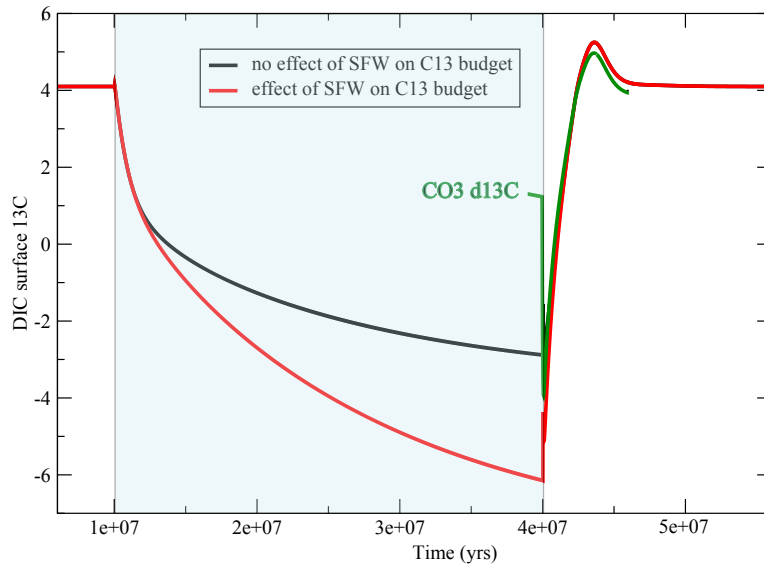


Fig. 9a. Modeled $\delta^{13}\text{C}$ profile during and aftermath the global glaciation. The blue bland represents the glaciation duration.

1873

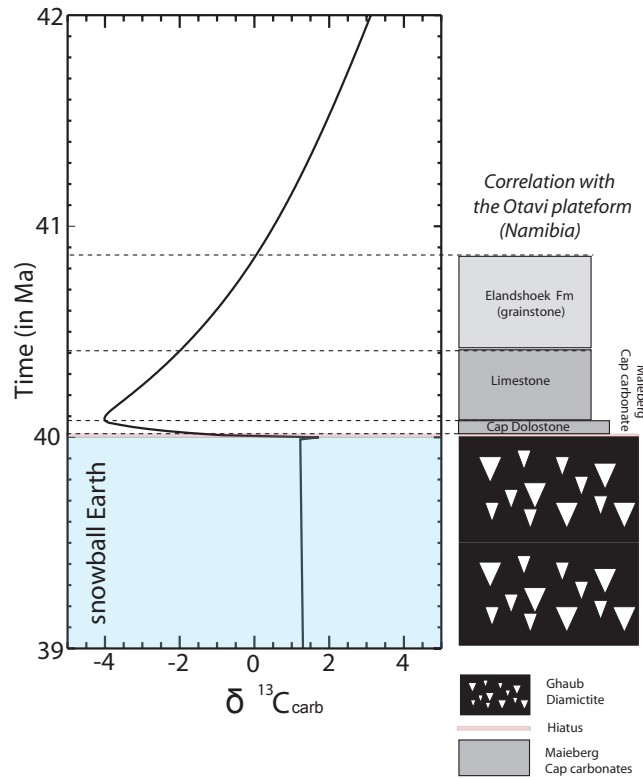


Fig. 9b. The comparison between modelled isotopic variations and isotopic records in Otavi Platform carbonates (Namibia). The blue bland represents the glaciation duration.

1874

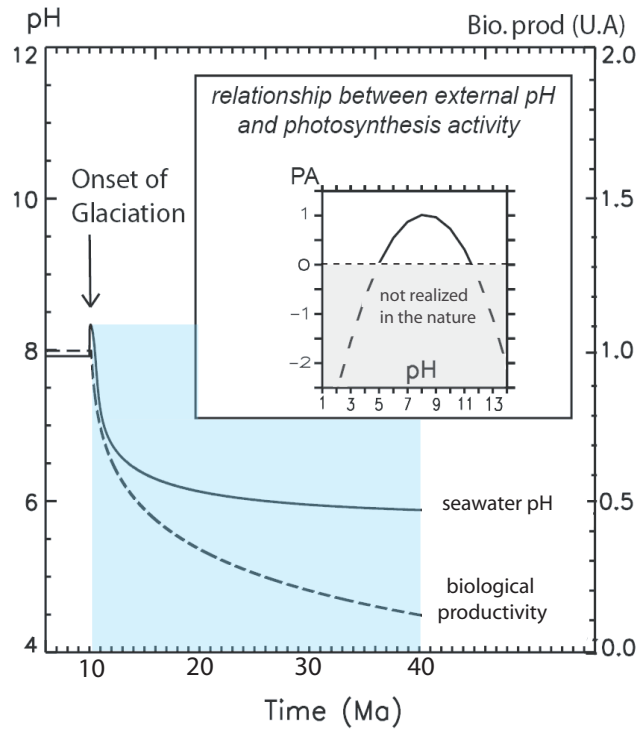


Fig. 10. Photosynthetic activity as function of a long-lived acidification of seawater. The blue bland represents the glaciation duration.

1875

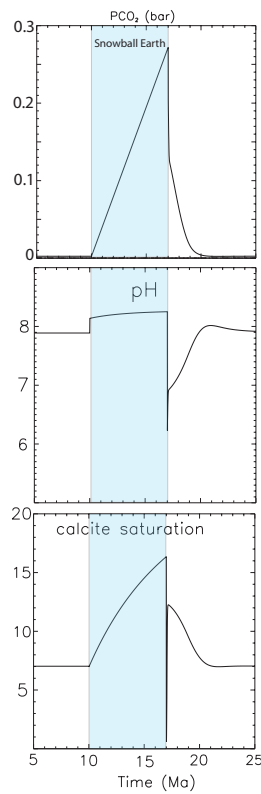


Fig. 11. Seawater modifications with an ocean isolated from the atmosphere. The blue bland represents the glaciation duration.

1876